Focus: Structure and dynamics of the interfacial layer in polymer nanocomposites with attractive interactions

Shiwang Cheng, Bobby Carroll, Vera Bocharova, Jan-Michael Carrillo, Bobby G. Sumpter, and Alexei P. Sokolov

Citation: The Journal of Chemical Physics **146**, 203201 (2017); doi: 10.1063/1.4978504
View online: http://dx.doi.org/10.1063/1.4978504
View Table of Contents: http://aip.scitation.org/toc/jcp/146/20
Published by the American Institute of Physics

Focus: Structure and dynamics of the interfacial layer in polymer nanocomposites with attractive interactions

Shiwang Cheng,[1,a)] Bobby Carroll,[2] Vera Bocharova,[1] Jan-Michael Y. Carrillo,[3,4] Bobby G. Sumpter,[3,4] and Alexei P. Sokolov[1,2,a)]
[1]*Chemical Sciences Division, Oak Ridge National Laboratory, Oak Ridge, Tennessee 37831, USA*
[2]*Department of Physics and Astronomy, University of Tennessee, Knoxville, Tennessee 37996, USA*
[3]*Center for Nanophase Materials Sciences, Oak Ridge National Laboratory, Oak Ridge, Tennessee 37831, USA*
[4]*Computer Science and Mathematics Division, Oak Ridge National Laboratory, Oak Ridge, Tennessee 37831, USA*

(Received 5 December 2016; accepted 24 February 2017; published online 30 March 2017)

In recent years it has become clear that the interfacial layer formed around nanoparticles in polymer nanocomposites (PNCs) is critical for controlling their macroscopic properties. The interfacial layer occupies a significant volume fraction of the polymer matrix in PNCs and creates strong intrinsic heterogeneity in their structure and dynamics. Here, we focus on analysis of the structure and dynamics of the interfacial region in model PNCs with well-dispersed, spherical nanoparticles with attractive interactions. First, we discuss several experimental techniques that provide structural and dynamic information on the interfacial region in PNCs. Then, we discuss the role of various microscopic parameters in controlling structure and dynamics of the interfacial layer. The analysis presented emphasizes the importance of the polymer-nanoparticle interactions for the slowing down dynamics in the interfacial region, while the thickness of the interfacial layer appears to be dependent on chain rigidity, and has been shown to increase with cooling upon approaching the glass transition. Aside from chain rigidity and polymer-nanoparticle interactions, the interfacial layer properties are also affected by the molecular weight of the polymer and the size of the nanoparticles. In the final part of this focus article, we emphasize the important challenges in the field of polymer nanocomposites and a potential analogy with the behavior observed in thin films. *Published by AIP Publishing.* [http://dx.doi.org/10.1063/1.4978504]

I. INTRODUCTION

Polymer nanocomposites (PNCs) are widely used in many current technologies and have even greater potentials for a large number of future applications ranging from energy to biomedical fields.[1–5] Their main advantages are light-weight, easy processing, low cost, and more importantly the large tunability in macroscopic properties, including the mechanical, optical, electrical, thermal, and transport properties.[4–6] Depending on the PNC application, the macroscopic properties of nanocomposites can be either nanoparticles dominated or polymer dominated. For example, in PNCs with tunable optical and electric properties, the embedded nanoparticles possess certain properties, such as optical absorption and fluorescence,[7–9] and act as electronic conductors, like metal nanoparticles, carbon nanotubes, and graphene.[10,11] The polymer matrices in these cases provide advantage of flexibility and good processability.[7,8,10] In polymer nanocomposites with enhanced mechanical properties[12,13] and transport properties,[14] the influences of nanoparticles to the properties of polymer matrices become more significant.[15]

Despite their broad use, detailed understandings of microscopic parameters controlling macroscopic PNC's properties remain limited.[6] One of the main complications in this field is caused by the aggregation of nanoparticles,[16,17] which is difficult to control.[16–20] For example, recent studies show that similar samples produced in different laboratories can have strong differences in their macroscopic properties.[21,22] These discrepancies are known to be partially caused by the strong sensitivity of the dispersion to the nanoparticle pre-treatments, the solvents used, the process of nanoparticles and polymer mixing, and the succeeding solvent removal and annealing.[21,22]

Moreover, there is still significant confusion in the literature even for PNC samples with good nanoparticle dispersion.[23–28] For example, using fluorescence probe technique, the authors of Ref. 29 reported a ~15 K shift in the glass transition temperature T_g when only less than 0.5 vol. % of SiO_2 nanoparticles have been added to poly(2-vinyl pyridine) (P2VP). However, less than a 5 K shift in T_g was reported for the same P2VP/SiO_2 PNC with larger than 25 vol. % of nanoparticles from dielectric and differential scanning calorimetry (DSC) measurements.[25,30] This confusion, in our view, is caused by a conceptually incorrect question being asked in these studies since PNCs are intrinsically heterogeneous systems with a significant interfacial region between the nanoparticles surface and the bulk

[a)]Authors to whom correspondence should be addressed. Electronic addresses: chengs@ornl.gov and sokolov@utk.edu

polymer that exhibits distinct macroscopic properties from each component of PNCs.[31–33] In other words, the structure, mechanics, and dynamic properties of the polymer change with the distance from the nanoparticle surface.[31–37] Additionally, it has been shown that the polymer glass transition temperature can be different at the nanoparticle surface and in the bulk far from the interface.[24,25,38,39] In this respect, the field of PNCs is very similar to the field of thin polymer films where interfacial properties and their gradients as a function of distance from the surface play a critical role. This analogy between thin films and PNCs has been emphasized in many studies.[29,40]

Although the studies of PNCs can also help to better understand the properties of thin films, i.e., their gradients and the role of surfaces and interfaces, PNCs allow studies of the interfacial properties in bulk samples, providing much higher accuracy of measurements (assuming good dispersion of the nanoparticles). More importantly, PNCs have more practical applications than thin polymer films of tens of nanometers. According to the current understanding, the interfacial layer is a key to tuning macroscopic properties of PNCs.[3,4] Simple estimates suggest that in a PNC with volume fraction $\varphi_{NP} = 10$ vol. % loading of spherical nanoparticles of 10 nm in diameter and an interfacial layer thickness of ~5 nm, the interfacial region will occupy more than 75 vol. % of the polymer matrix. Thus, understanding microscopic parameters that control the structure and properties of the interfacial layer is critical for the design of PNCs with desired macroscopic properties, especially on the mechanical properties and transport properties of PNCs.[4]

In this article, we focus on analysis of the interfacial layer structure and dynamics in model nanocomposites with attractive polymer-nanoparticle interactions and well-dispersed spherical nanoparticles. First we summarize experimental methods and data analyses that provide characterization of the interfacial layer structure, dynamics, and mechanical properties of the PNCs. Then we use the data from these studies to unravel the role of polymer structure and polymer-nanoparticle interactions to the properties of the interfacial layer. This analysis is based mostly on experimental studies that were combined with results of computer simulations and theory. At the end, we will outline some important future directions that might help develop a deeper understanding of the parameters that control the interfacial regions and macroscopic properties of PNCs.

II. EXPERIMENTAL STUDIES OF THE INTERFACIAL REGION IN PNCs

For quantitative studies, it is important to have samples with well-dispersed nanoparticles. One of the traditional ways to analyze the dispersion is to use transmission electron microscopy (TEM) imaging. Nanoparticle aggregates are usually visible in TEM. The disadvantage of TEM imaging is that only a relatively small part of the sample is analyzed, meaning that there are no ensemble averaged parameters. A better technique is small angle X-ray scattering (SAXS) or small angle neutron scattering (SANS) that provide an ensemble averaged distribution of nanoparticles and their aggregates.[41–44]

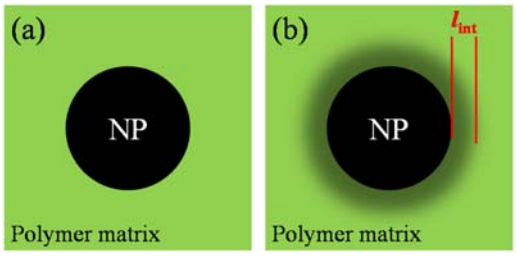

FIG. 1. (a) A sketch for the two phase model (TPM) that is composed of the nanoparticles (NP) and homogeneous polymer matrix. (b) A sketch of the interfacial layer model (ILM) with an additional component, the interfacial layer surrounding the nanoparticles. The thickness of the interfacial layer is l_{int}.

Two approaches can be used in the analysis of the experimental data in PNCs. The two phase model (TPM) assumes nanoparticles in a homogeneous matrix (Fig. 1(a)), and the properties are analyzed as a particular combination of the properties of these two phases. In most cases, however, the TPM approach fails to describe the PNC properties, and an interfacial layer model (ILM) has to be involved (Fig. 1(b)). This model assumes that in addition to nanoparticles and matrix there is an interfacial layer with polymer properties different from the properties of the matrix. In Secs. II A–II F, we will describe how the interfacial layer is characterized by a variety of experimental techniques, and how an interfacial layer model (ILM) is used to help better understand the data.

A. Small-angle scattering measurements of the interfacial layer

Small angle x-ray scattering (SAXS) and small angle neutron scattering (SANS) techniques are sensitive to the changes in the scattering length density (SLD) that usually differs strongly for the polymer matrix and nanoparticles.[45] This difference produces scattering patterns that are distinguishable from the spectra of the neat polymer matrix and provides information on nanoparticles' size and dispersion (Fig. 2). The SLD also changes with variations of the material's mass density.

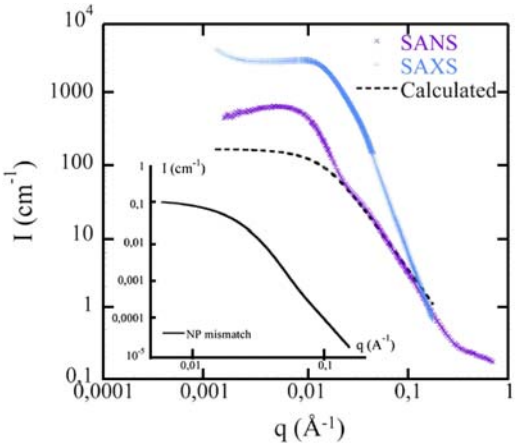

FIG. 2. SAXS and SANS for PMMA/SiO_2-30 vol.%. The dashed line is a theoretical calculation of the scattering intensity due to the mismatch of the scattering length density (SLD) of the silica and PMMA matrix (the TPM model). The inset shows the calculated form factor of nanoparticles (NP) in PMMA/SiO_2 PNCs using the experimental SLD difference from measured results. Reprinted with permission from Jouault *et al.*, ACS Macro Lett. **5**(4), 523–527 (2016). Copyright 2016 American Chemical Society.

As a result, additional scattering will appear if the density of the polymer changes in the vicinity of the nanoparticles. In some cases, the TPM model (usually called the hard sphere model in scattering analysis) appears sufficient to describe SAXS or SANS data.[46,47] This usually indicates rather small variations in the polymer density in the interfacial region. However, in most cases a polydisperse core-shell model (a kind of ILM) should be used to accurately describe the SAXS/SANS data[25,36,43,44,46,47] (Fig. 2). It reflects a measurable difference in density of the matrix and that of the interfacial layer. Surprisingly, it was revealed that the density of the interfacial layer in many cases appears to be lower than the density of the bulk polymer matrix.[43,47] These measurements were able to provide estimates of the interfacial layer thickness as well, with $l_{int} \sim$ 2-5 nm.[25,36,44,46,47] These data sets produce estimates of the length scale by interpreting changes in mass density in the interfacial region, i.e., they give an estimate of the static interfacial layer thickness, l_{int}.

B. Nuclear Magnetic Resonance (NMR) measurements of the interfacial dynamics in PNCs

Historically, the presence of the dynamically immobilized region at the rubber/carbon black interface, in contrast to the dynamics of the free rubber matrix, was first discovered by Kaufman *et al.*[48] based on Nuclear Magnetic Resonance (NMR) measurements. By measuring the spin-spin relaxation time (T_2) of *cis*-polybutadiene/carbon black and ethylene-propylene-diene rubber/carbon black, the authors were able to identify two different relaxation regions that are distinct from the neat rubber, an immobilized region and a relatively mobile region, although both regions exhibit strong slowing down in comparison to the neat rubber.[48] The immobilized region was assigned to the bounded rubber layer on the carbon black. More importantly, these authors further estimated the volume fraction of the immobilized region at different temperatures for the two different types of rubber/carbon black composites. For a given surface contact area between rubber and carbon black, their measured temperature dependence of the volume fraction of the immobilized rubber can be taken to be the earliest measurements of the temperature dependence of the interfacial layer thickness in composite materials.

Later, Berriot *et al.*[49] applied the same technique to crosslinked poly(ethyl acrylate)/SiO_2 nanocomposites with surface modified nanoparticles to improve the dispersion of nanoparticles. They also found regions with different segmental mobility in the PNCs with both covalently bonding hairy nanoparticles and in systems with physically absorbed chains.[49] Since the average segmental relaxation time of the immobilized region agreed well with the relaxation time of the matrix measured at $T \sim T_g^{NMR}$, the authors assigned this layer to a glassy layer surrounding the nanoparticles. The thickness of the "glassy" layer and its temperature dependence were also presented in their original paper (Fig. 3).

More recent NMR studies of poly(ethylene glycol) (PEG)/SiO_2 nanocomposites also support the existence of a "glassy" layer surrounding the nanoparticles. Instead of the conventional ILM model (Fig. 1(b)), they introduced a more complex picture (Fig. 4): (i) a glassy layer, (ii) an immobilized layer, and (iii) a bulk matrix.[24,50] Thus NMR studies can provide estimates of two dynamically distinct interfacial layer thicknesses: thickness of the "glassy" layer and thickness of the "immobilized" layer with dynamics slower than the dynamics of the polymer matrix.

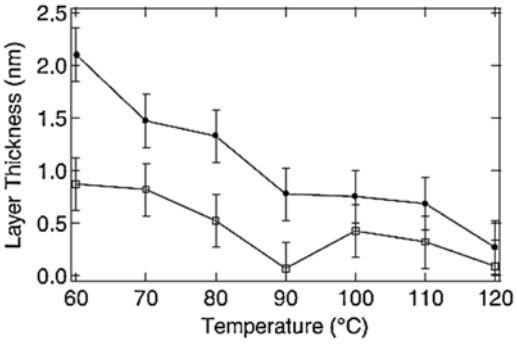

FIG. 3. Temperature dependence of the "glassy" layer thickness of the crosslinked poly(ethyl acrylate)/SiO_2 PNCs from H-NMR for polymer matrix covalently bonding to the nanoparticles (filled symbols) and for polymer matrix physically adsorbed onto the surface of nanoparticles (empty symbols). Reprinted with permission from Berriot *et al.*, J. Non-Cryst. Solids **307–310**, 719–724 (2002). Copyright 2002 Elsevier.

C. Mechanical measurements of PNCs

The signature of the interfacial layer has also been found from dynamic mechanical measurements. For example, Tsagaropoulos and Eisenburg[51,52] have carried out a set of dynamic mechanical measurements on polymer/silica composites with different polymer matrices, including poly(vinyl acetate) (PVAc), polystyrene (PS), poly(meth methacrylate) (PMMA), and poly(4-vinylpyridine) (P4VP). Two features are found in nanocomposites (Fig. 5): (i) a reduction in the glass transition peak amplitude in tan δ; (ii) a appearance of an additional dissipation peak in tan δ at high temperatures. The authors assigned these features to the presence of strongly absorbed interfacial polymers on the surface of nanoparticles that have a much higher glass transition than the neat polymers.

Unfortunately, although these mechanical measurements suggested a clearly separate T_g associated with the interfacial

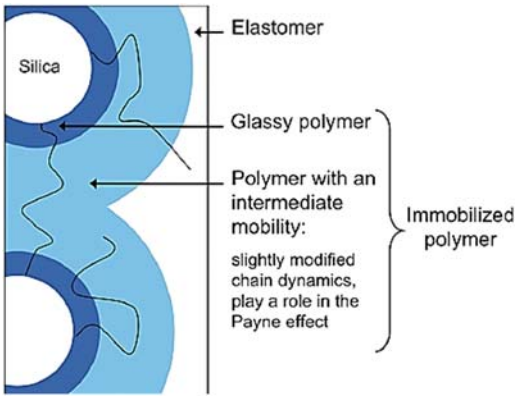

FIG. 4. The three-layer model proposed by Papon *et al.*[24] that includes a glassy layer, an intermediate mobility layer, and a bulk layer with high mobility. The combination of the glassy layer and the intermediate mobility layer is also called the immobilized polymer layer. Reproduced with permission from Papon *et al.*, Soft Matter **8**(15), 4090–4096 (2012). Copyright 2012 The Royal Society of Chemistry.

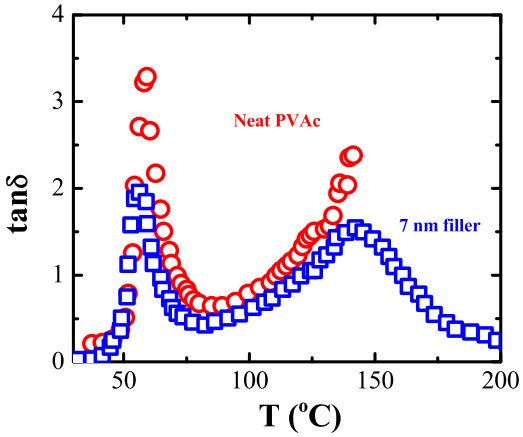

FIG. 5. Dynamic mechanical measurements (tan δ) at $f = 0.33$ Hz of the neat PVAc (red circles) and PVAc/silica-10 wt. % composites with nanoparticles of 7 nm in diameter (blue squares). The first peak indicates the glass transition peak of the neat PVAc (or free PVAc in the case of composites). An additional peak appears in the nanocomposites, signifying a much higher glass transition temperature of the adsorbed polymers, i.e., polymers in the interfacial region. Reprinted with permission from G. Tsagaropoulos and A. Eisenburg, Macromolecules **28**(1), 396–398 (1995). Copyright 1995 American Chemical Society.

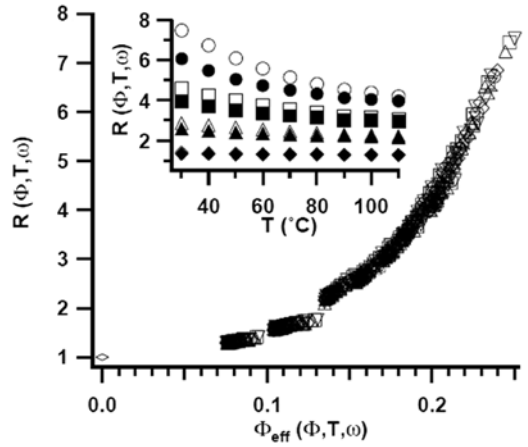

FIG. 6. Master curves of the reinforcement factor of the nanocomposites, $R(\Phi, T, \omega) = G_{PNC}(\Phi, T, \omega)/G_{neat}(T, \omega)$, as a function of the effective nanoparticle loading, $\Phi_{eff}(\Phi, T, \omega) = \Phi + \varphi_{glassy}(T)$, where $G_{PNC}(\Phi, T, \omega)$ is the shear modulus of the nanocomposites of volume fraction, Φ, at temperature, T, and frequency, ω; $G_{neat}(T, \omega)$ is the shear modulus of the neat polymer at temperature, T, and frequency, ω; $\varphi_{glassy}(T)$ is the volume fraction of the glassy layer at temperature T. The inset shows the reinforcement factor as a function of temperature for poly(ethyl acrylate)/SiO_2 nanocomposites of different volume fractions and different frequencies:○ 17.7 vol. %, 10 Hz; • 17.7 vol. %, 0.01 Hz; □ 15 vol. %, 10 Hz; ■ 15 vol. %, 0.01 Hz; Δ 12 vol. %, 10 Hz; ▲ 12 vol. %, 0.01 Hz; ◇ 6.7 vol. %, 10 Hz; ♦ 6.7 vol. %, 0.01 Hz. Data are from Berriot *et al.*, "Gradient of glass transition temperature in filled elastomers," Europhys. Lett. **64**(1), 50 (2003). Copyright 2003 European Physical Society.

polymer, the volume fraction of the interfacial layer cannot be directly estimated from the dynamic mechanical measurements. The modulus of the interfacial layer is expected to be higher, which is critical to the overall mechanical enhancement in polymer nanocomposites. Recently, Berriot *et al.*[39] took advantage of the thickness estimate from the NMR measurements to better understand the linear viscoelasticity of the PNCs. Remarkably, by taking into account the finite thickness of the interfacial layer with a glassy modulus, the authors proposed a new specific temperature-frequency superposition law that explained the linear viscoelasticity of PNCs with different loadings fairly well[38,39] (Fig. 6). A similar strategy has been followed by Papon *et al.* who incorporated the thickness of the glassy layer and the immobilized layer from NMR measurements to explain the linear viscoelasticity and even the Payne effect of PNCs.[24]

Atomic force microscopy (AFM) can also be applied to probe the local mechanical properties of the interface in the polymer nanocomposites. For example, nano-indentation can provide the surface modulus of polymer nanocomposites with a spatial resolution down to ~1-10 nm. Since the interfacial layer is thought to be "glassy" and possess significantly higher (10^2-10^3 times) modulus than the bulk rubbery polymer, the AFM should be sensitive enough to detect it. Indeed, an interfacial layer with a higher modulus as well as the gradient of that modulus can be directly mapped out.[36,53–57] These measurements absolutely confirm the presence of a new mechanically different interphase in composite material as well as in thin polymer films. However, the reported value of the thickness of this interphase is very scattered ranging from a few nanometers to tens of nanometers. Such inconsistency might be related to intrinsically very different nature of studied materials or to challenges in collecting and analyzing AFM data. The outcome of the AFM measurements are also strongly affected by the size and shape of the tip, the mode applied, the local geometry at the polymer/nanoparticle interface,[57] and the model used for data treatment.

Brillouin light scattering (BLS) is another method that can measure the high frequency mechanical modulus, including the shear and longitudinal moduli (from which the bulk and Young moduli can be also estimated). For PNCs with inorganic nanoparticles, a clear mechanical enhancement can be observed from the large blue shift in characteristic frequencies of the transverse and longitudinal waves.[22,36,58,59] However, a TPM approach, with assumption that no changes occur in the mechanical properties of the polymer, cannot describe the mechanical data of PNCs in both rubbery and glassy states. The deviation is significant, especially at high loadings (Fig. 7),

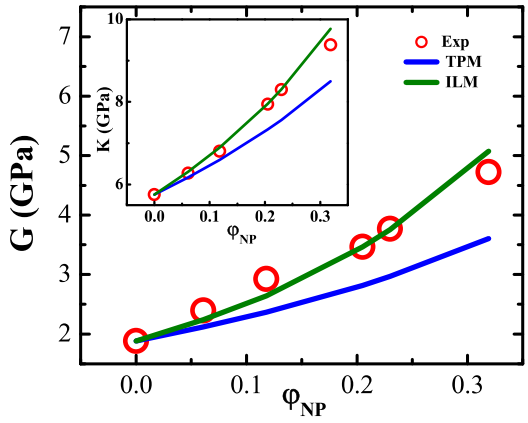

FIG. 7. Shear modulus, G, and bulk modulus (inset), K, of PVAc/SiO_2 nanocomposites of different loadings (radius of nanoparticle R_{NP} = 12.5 nm, φ_{NP} = 0 vol. %–31.9 vol. %) measured by depolarized Brillouin light scattering at T = 213 K. The bulk lines are prediction of the TPM model and the green lines are the predictions of the ILM model by assuming the l_{int} = 3 nm. Detailed calculations of the mechanical response of PNCs based on the TPM, and ILM mechanical model can be found in Ref. 36. Reprinted with permission from Cheng *et al.*, Nano Lett. **16**(6), 3630–3637 (2016). Copyright 2016 American Chemical Society.

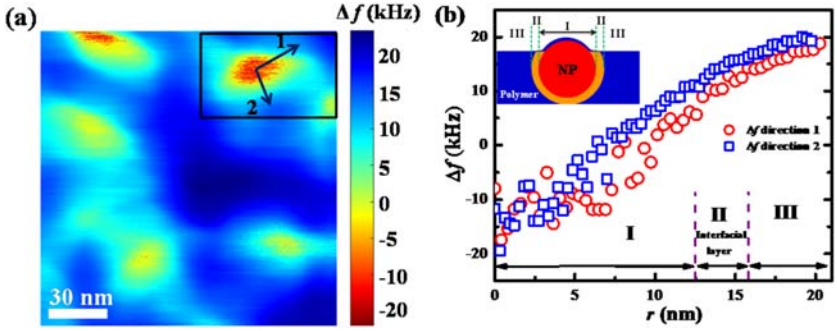

FIG. 8. (a) Resonance frequency shift (Δf) map of the surface of the PVAc/SiO_2-23 vol. % (R_{NP} = 12.5 nm) measured by AFM. The red and yellow islands represent the hard bare nanoparticles and the embedded nanoparticles, respectively, and the blue regions represent the neat polymer. The cyan shell between the nanoparticles and the polymer matrix region is the interfacial layer. (b) The gradient profile of the Δf in terms of the distance, r, from the center of the nanoparticle along the directions 1 and 2 indicated by the black arrows in panel (a). The inset (b) shows the schematic positioning of the nanoparticle in the polymer matrix. Three regions associated with different changes in Δf can be assigned. Reprinted with permission from Cheng *et al.*, Nano Lett. **16**(6), 3630–3637 (2016). Copyright 2016 American Chemical Society.

indicating the presence of an interfacial layer with enhanced mechanical modulus.[36,53,58] In particular, the recent studies[36] using the ILM approach and independently estimated thicknesses of the interfacial layer revealed that even in the glassy state the shear modulus of the interfacial layer is more than 2 times higher than that of the polymer matrix. Using an advanced AFM technique, the authors were also able to image the interfacial layer in glassy PNCs (Fig. 8), and estimated its thickness to be ~3 nm in PVAc/SiO_2 PNC.

D. Broadband dielectric spectroscopy studies of PNCs

Broadband dielectric spectroscopy (BDS) provides information on dynamics and relaxation processes in an extremely broad frequency range, usually from 10^{-3}-10^{-2} Hz to 10^{7}-10^{9} Hz. It measures the reorientation of depolarized dipole moments as well as ion conductivity.[60] The main advantages of BDS are a broad frequency range and a high accuracy of the measurements that allow for careful interpretation by various models. Polymer segmental relaxation (α-relaxation) appears as a peak in the dielectric loss spectra ε″(ω) (Fig. 9). The angular frequency, ω, of its maximum provides estimates of the characteristic segmental relaxation time $\tau_\alpha = 1/(\omega_{max})$, while the integrated amplitude provides an estimate of the fraction of the polymer with this segmental relaxation. Adding nanoparticles to a polymer matrix brings several noticeable changes in the BDS spectra (Fig. 9): (1) a reduction in alpha peak intensity; (2) a broadening; (3) a shift to lower frequencies in the alpha peak; (4) an additional Maxwell-Wagner-Sillars (MWS) process in the lower frequency ranges; and (5) a shift in the dc-conductivity. The dc-conductivity can either increase or decrease, depending on the amount of impurities or ions introduced during the sample preparation.

Different approaches are proposed to analyze the dielectric spectra of the nanocomposites. For example, Gong *et al.*[26] fit the loss spectra with one process with particular restrictions

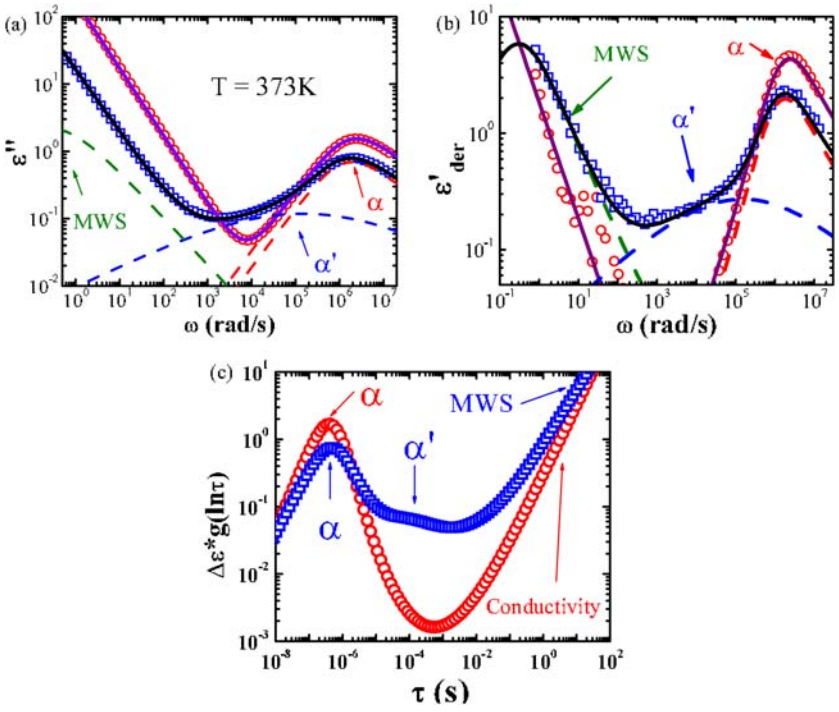

FIG. 9. Dielectric loss spectra (a), ε″ (ω), dielectric derivative spectra (b), $\varepsilon'_{der}(\omega) = -\pi/2 * \partial\varepsilon'(\omega)/\partial \ln\omega$, and relaxation time distribution spectra (c), $\Delta\varepsilon * g(\ln\tau)$, of PVAc/$SiO_2$-20.5 vol. % ($R_{NP}$ = 12.5 nm) (blue squares) and neat PVAc (red circles) at T = 373 K. The solid lines are the fit of the Havriliak-Negami function plus dc-conductivity for the neat PVAc, and the ILM model for PVAc/SiO_2-20.5 vol. %. The detailed fit procedure of the ILM model for dielectric spectra can be found in Ref. 31. The red dashed lines represent the dielectric functions of the neat PVAc. The green dashed lines represent the dielectric contribution from the Maxwell-Wagner-Sillars (MWS) polarization. A clear interfacial layer process, α′ with a slowing down in characteristic relaxation times can be identified from each spectra. Data were replotted from Cheng *et al.*, Phys. Rev. Lett. **116**(3), 038302 (2016). Copyright 2016 The American Physical Society.

on the spectral shape parameters of the fit function; however, the analysis only covered a limited amount of the frequency range of the alpha peak. They assigned this peak to the volume fraction of the free polymer matrix, and the remaining volume fraction was assigned to the interfacial layer. The volume fraction of the interfacial layer can be estimated from $\varphi_{int} = 1 - \varphi_{NP} - \Delta\varepsilon_{PNC}/\Delta\varepsilon_{PVAC}$, where the last term corresponds to the estimated volume fraction of the bulk polymer matrix. It is worth noting that this approach does not provide any dynamic information on the interfacial layer, usually fails to fit the entire broad frequency range spectra, and underestimates the thickness of the interfacial layer.

A more prevailing method, the additive approach, is to assume additional contribution, i.e., a separate dielectric process associated with the interfacial layer, and fit the spectra with two peaks described by the Havriliak-Negami function,[25,61–63]

$$\varepsilon^*(\omega) = \varepsilon_\infty + \frac{\Delta\varepsilon_{bulk}}{[1 + (i\omega\tau_{HN}^{bulk})^{\alpha_1}]^{\gamma_1}} + \frac{\Delta\varepsilon_{\text{int}}}{[1 + (i\omega\tau_{HN}^{\text{int}})^{\alpha_2}]^{\gamma_2}} - i\frac{\sigma}{\varepsilon_0\omega},$$

where $\varepsilon^*(\omega)$, ε_∞, $\Delta\varepsilon$, ε_0, ω, τ, and σ are the complex dielectric function of the polymer nanocomposites, the dielectric constant at infinite high frequency limit, the dielectric strength of a corresponding relaxation process, the vacuum dielectric constant, the angular frequency, the characteristic relaxation time of the process, and the dc-conductivity of PNCs, respectively. The i is the imaginary unit. α and γ are the shape parameters of the corresponding process. The *bulk* and *int* indices correspond to the bulk polymer matrix and interfacial layer, respectively. The shape of the bulk peak is usually assumed to be the same as in the neat polymer, and only its relaxation time and amplitude are varied in the fit. From this fitting, the interfacial layer fraction can be estimated as $\varphi_{\text{int}} = (1 - \varphi_{NP}) \times \frac{\Delta\varepsilon_{\text{int}}}{\Delta\varepsilon_{\text{int}} + \Delta\varepsilon_{bulk}}$. This method provides characteristic relaxation times as well as the thickness of the interfacial layer.

However, the additive approach ignores the heterogeneous nature of the nanocomposite materials which results in additional interference terms in the dielectric response functions of PNCs.[31,60,64,65] In contrast, the heterogeneous model analysis approaches explicitly calculate the dielectric response of the multicomponent systems based on the geometries of TPM and ILM. Thus, they take into account the dielectric response of each component as well as the interference terms between different components. For details of this approach we refer the reader to old[64] and recent papers[31,46,47] which suggest a way for more accurate treatment of the dielectric spectra of composite materials. This heterogeneous model analysis approach provides rather accurate estimates of characteristic segmental relaxation time and volume fraction, φ_{int}, of the interfacial layer in a broad temperature range.[31] The thickness of the interfacial layer can then be estimated from φ_{int}: $l_{\text{int}} = R_{NP}\left(\left(\frac{\varphi_{\text{int}} + \varphi_{NP}}{\varphi_{NP}}\right)^{1/3} - 1\right)$, where R_{NP} is the radius of the nanoparticles. Thus BDS provides accurate estimates of the temperature dependence of the interfacial layer thickness, and a detailed analysis of its dynamics. These detailed studies suggested that there are no "glassy" or "dead" layers in studied PNCs, at least in any significant amount.[31,46,47] Instead, the segmental dynamics of the interfacial layer appears to have a broad distribution of relaxation times (or corresponding glass transition temperatures).

E. Quasielastic neutron scattering studies of PNCs

Other than H-NMR and BDS, quasielastic neutron scattering (QENS) techniques also have been used to study the dynamics of the polymer nanocomposites.[66–70] An advantage of neutron scattering is the possibility to study microscopic details of the dynamics, not only characteristic relaxation times but also geometry of the underlying motions. However, QENS can measure dynamics only faster than a few hundreds of nanoseconds and does not cover a very broad time (or frequency) range. Several studies focused on the analysis of nanoparticles and chain diffusion in PNCs[68–70] and revealed significant slowing down of chain diffusion. A few papers also analyzed segmental dynamics in PNC and revealed two populations of the segmental dynamics:[66,67] one that has dynamics of the bulk polymer and another one with significantly slower dynamics. Using these results, the thickness of the interfacial layer was estimated to be ~5 nm in PDMS/SiO_2 nanocomposite.[67] We also want to mention a recent QENS study of polymer dynamics in confinement.[37] The authors clearly demonstrate the absence of the "immobile" or "glassy" layer. Instead, they found that the dynamics is slowed down in the interfacial layer due to attractive chain-wall interactions.

F. Differential scanning calorimetry studies of PNCs

Differential scanning calorimetry (DSC) is a well-known technique to estimate the glass transition temperature as a step in the thermodynamic function. It has been realized that this technique can also probe thermodynamics characteristics of the interfacial layer.[30,71] For example, Sargsyan *et al.*[71] analyzed the specific heat capacity of nanocomposites with different loadings. The ratio of the specific heat capacity jump of nanocomposites and the specific heat capacity of the neat polymer provides an estimate of the volume fraction of the mobile polymers in nanocomposites.[71] According to these authors, the interfacial layer is a thermodynamically "dead" layer with no characteristics in the DSC curves even at extremely high temperatures.[71] However, these analyses typically ignored the specific heat capacity change of the silica nanoparticles within the glass transition temperature step of the PNCs. Recently, Holt *et al.*[25] proposed a more rigorous analysis that normalizes the specific heat capacity of the polymer matrix by the mass fraction of the polymer matrix:[25,31,46,47,72] $C_p^{mat} = \frac{C_p^{PNC} - C_p^{NP} m_{NP}}{1 - m_{NP}}$, where C_p^{mat}, C_p^{PNC}, and C_p^{NP} are the specific heat capacity of the polymer matrix, the polymer nanocomposites, and the nanoparticles, respectively, and the m_{NP} is the mass fraction of the nanoparticles. As shown in Fig. 10, the total normalized specific heat capacity jump of the polymer matrix is identical to the neat polymer matrix and is rather independent of nanoparticle loading, indicating the absence of a "dead" layer in PNCs. However, the glass transition step of the nanocomposites significantly broadens and ends up at a much higher temperature than the T_g of the neat matrix. This broadening clearly indicates the presence of an interfacial layer with slower dynamics and higher T_g. The authors of Ref. 73 proposed using the fraction of the tail in DSC step to estimate

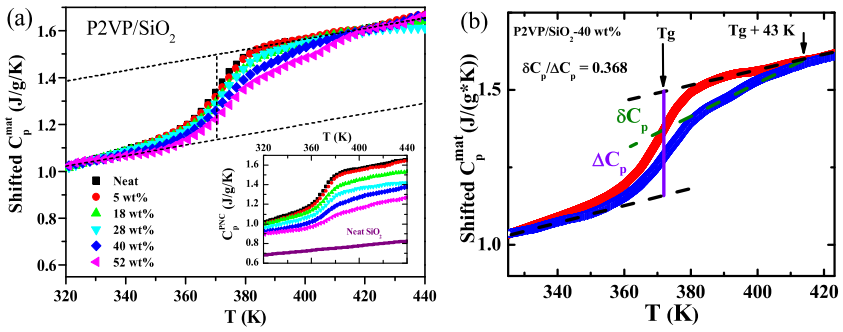

FIG. 10. (a) Shifted specific heat capacity of the matrix polymer, C_p^{mat}, of P2VP/SiO_2 (R_{NP} = 15 nm) of different mass loadings m_{NP} = 5 wt. %–52 wt. %. The inset shows experimental raw data of C_p^{PNC}, where the solid purple line represents the specific heat capacity of neat silica nanoparticles in the same temperature range. Significant broadening is found in the glass transition step in PNCs, where the glass transition of PNCs ends up at a much higher temperature compared with neat P2VP. No signs of a "dead" layer have been observed. Reprinted with permission from Holt *et al.*, Macromolecules **47**(5), 1837–1843 (2014). Copyright 2014 American Chemical Society. (b) Representative analysis of the differential scanning calorimetry data of P2VP/SiO_2–40 wt. % (R_{NP} = 15 nm), where the specific heat capacity of the neat P2VP is ΔC_p during the glass transition, and the specific heat capacity associated with the broadening tail in PNC is δCp. The interfacial layer is l_{int} = 3.4 nm in the case of P2VP/SiO_2-40 wt. % (R_{NP} = 15 nm).

the fraction of the interfacial layer from the thermodynamics measurements (Fig. 10): $\varphi_{int} = (1 - \varphi_{NP})\delta C_p/\Delta C_p$, with $l_{int} = R_{NP}\left(\left(\frac{\varphi_{int}+\varphi_{NP}}{\varphi_{NP}}\right)^{1/3} - 1\right)$ where δC_p is the specific heat capacity associated with the broadening tail and ΔC_p is the specific heat capacity of the neat polymer at the glass transition (Fig. 10(b)).

III. MICROSCOPIC PARAMETERS CONTROLLING STRUCTURE AND DYNAMICS OF THE INTERFACIAL LAYER IN PNCs

The experimental techniques described above provide estimates of the interfacial layer thickness, dynamics, and mechanical moduli of polymer nanocomposites. Moreover, they allow one to analyze the temperature dependence of these parameters. As we already mentioned, due to the large volume fraction of nanoparticles and significant volume fraction of the interfacial layer in PNC samples, very accurate and detailed studies of the interfacial properties can be performed. Here, we will focus on the role of microscopic parameters in defining the properties of the interfacial layer of PNCs. These parameters include nanoparticle-polymer interactions, nanoparticle size, polymer chain rigidity, and molecular weight.

A. Influence of nanoparticle—Polymer interactions

It is obvious that the strength of the nanoparticle-polymer interactions and whether it is attractive or repulsive will strongly affect the structure and dynamics in the interfacial region.[33,34,74–76] However, it is very difficult to analyze the influence of the interactions experimentally.[76–79] First of all, tuning interactions by changing polymer chemical structure causes variations in many other parameters, making it difficult to disentangle the effects. Surface modifications of nanoparticles that will affect the polymer-nanoparticle interactions usually lead to changes in their dispersion.[27,41,80,81] It is essentially impossible to disperse nanoparticles with repulsive interactions. Thus the main studies used to understand the role of strength of the interactions are done using MD-simulations,[33–35,74,75,82–84] especially given the limited experimental efforts on this topic.[76] Thus, we focus on the computer simulation results in this section since tuning the strength of interactions in a broad range without affecting other system parameters is relatively easy in simulations. Further, the conclusions of computer simulations from different research groups are more or less the same.

Several simulations studies demonstrated[32,33,35] that an increase in strength of the nanoparticle-polymer interactions leads to an increase in density in the interfacial layer, and also to a strong slowing down of the relaxation times at the interface (Fig. 11). Moreover, it also leads to an increase in steepness of the temperature dependence of segmental dynamics (fragility) in the interfacial layer in comparison with that of the neat polymer.[33,34] In the case of repulsive interactions (less favorable than polymer-polymer interactions), dynamics in the interfacial layer appears to be faster than in the neat polymer.[33,34,74,75] However, these studies also revealed that the thickness of the interfacial layer does not change appreciably with the change of the interaction strength.[33–35,74,75,82] In Figure 11, we show new results from simulations of Ref. 35 where we considered only flexible polymer chains in contact with an attractive surface having different short-ranged wall-to-polymer interaction

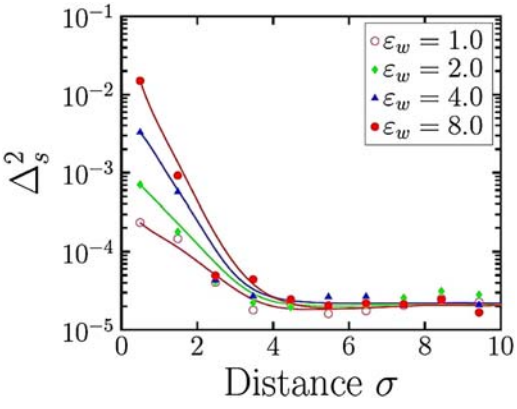

FIG. 11. Variance of the intermediate collective dynamic structure factor, Δ_s^2, at q = 6.15 σ^{-1} for flexible polymers in contact with a surface located at distance 0 σ with different short-ranged wall-to-polymer interaction strength, ε_w (in units of thermal energy, $k_B T$). All four data sets show a similar transition point (distance ~ 5 σ) where the surface cease to influence the collective dynamic structure factor, $S_{col}(q,t,z)$, and polymer segmental dynamics is bulk-like. See Ref. 35 for the details of the calculation and simulations.

strengths. The simulation shows that at a distance of around 5σ from the surface, the distance dependent intermediate collective dynamic structure factor, $S_{col}(q, t, z)$, with length-scales measured commensurate with the bead size σ (q = 6.15 σ^{-1}), transitions from being influenced by the surface and that of being statistically indistinguishable from bulk. Similar transition point is seen in Figure 11 for data sets having different wall-to-polymer interaction strengths.

B. Role of nanoparticle size

The curvature of the nanoparticle surface, i.e., the radius of the nanoparticle R_{NP} might also play a role in determining properties of the interfacial region.[85–87] This effect should be especially strong when R_{NP} becomes comparable or even smaller than the chain radius of gyration R_g.[3] Indeed, BDS studies of P2VP/SiO_2 nanocomposites with nanoparticle sizes in the range from R_{NP} = 7 nm to R_{NP} = 50 nm revealed an increase in the interfacial layer thickness (Fig. 12).[26] Although the overall volume fraction of the interfacial region decreased with the increase in R_{NP} at constant loading, this decrease was weaker than the expected decrease in the surface area of nanoparticles, clearly indicating an increase in l_{int} (Fig. 12). As we discussed in Section II D, the approach that the authors of Ref. 26 used in the analysis of the BDS data underestimates the interfacial volume fraction. In any case, the authors attributed the decrease in the interfacial layer thickness to a faster relief of the nano-confinement in the case of smaller nanoparticles. For example, by assuming a constant amount of segments affected by a unit surface area of nanoparticles, the authors formulated a very simple arguments on the effect of nanoparticle curvature, the radius R_{NP}, to the bound layer thickness, $\delta(R_{NP}) = (3R_{NP}^2\delta_\infty + R_{NP}^3)^{1/3} - R_{NP}$, where δ_∞ is the bound layer thickness for a flat surface. By assuming $\delta_\infty = l_k \sim 1.5$ nm for P2VP, the authors observed a reasonably good agreement between their model and experimental data for different PNCs (the solid lines in Fig. 12). Interestingly, this simple model suggests a saturation of the interfacial layer thickness at radii larger than 10 nm as shown by the solid lines in Fig. 12, which was independently observed by Papon *et al.*[76] and recently confirmed by computer simulations.[88] Unfortunately, this study only focused on the interfacial layer thickness at one temperature T = 130 °C. There were no temperature dependence of l_{int}, and no dynamics of the interfacial layer have been provided. In the future, it would be interesting to study how the average interfacial layer's slower dynamics changes with nanoparticle sizes, and how the interfacial layer thickness changes with temperature for different particle sizes.

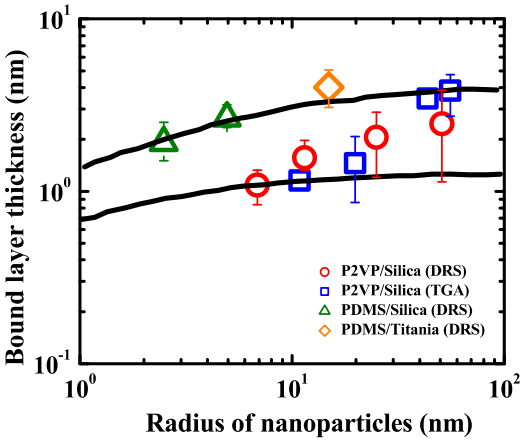

FIG. 12. Bound layer thickness, $\delta(R_{NP})$, with respect to the radius of nanoparticle, R_{NP}. The solid lines are predictions from the following equation: $\delta(R_{NP}) = (3R_{NP}^2\delta_\infty + R_{NP}^3)^{1/3} - R_{NP}$, where δ_∞ is the bound layer thickness for a flat surface. For PNCs with different polymer matrices, the $\delta_\infty \sim l_k$ (the Kuhn length of the polymer) is assumed. Note the red circles data points use the one Havriliak-Negami analysis that always underestimates the interfacial layer thickness, while the triangle and diamond points are results analyzed by additive methods. Adapted with permission from Gong *et al.*, ACS Macro Lett. **3**(8), 773–777 (2014). Copyright 2014 American Chemical Society.

C. Role of polymer chain rigidity

Chain rigidity is an obviously important molecular parameter that might affect the structure and dynamics of the interfacial region. The characteristic ratio, C_∞, is often used to define the chain rigidity.[89,90] Experimentally, it is almost impossible to find a set of different PNCs with systematic changes in the chain rigidity while keeping the same polymer-nanoparticle interactions. However, computer simulations can do this in a relatively simple way. For example, a recent study[35] analyzed the changes in the interfacial region caused by varying the coarse-grained chain bending potential at fixed polymer-wall interactions. They revealed significant influence of chain rigidity on structure, dynamics, and thickness of the interfacial region.[35] In general, computer simulations have shown that increasing polymer rigidity at fixed surface affinity leads to an increase in the number of adsorbed chain segments (*trains*), which improves surface packing of segments and results in slower dynamics.[35,91–94] More importantly, they found a good correlation between the chain rigidity and the thickness of the interfacial layer measured through static (e.g., density) and dynamic (structural relaxation time) properties (Fig. 13).

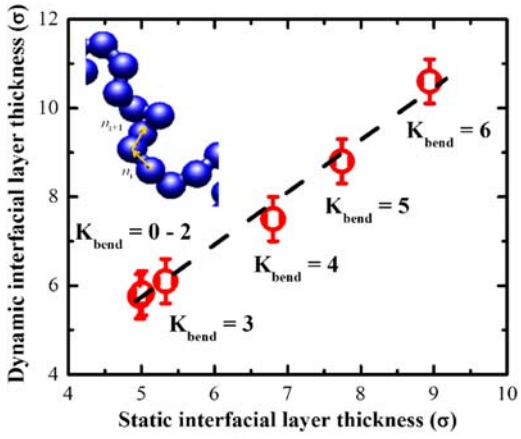

FIG. 13. A replot of the correlation between the dynamic interfacial layer thickness and the static interfacial layer thickness from a recent simulation.[35] The inset cartoon shows a part of the polymer chain under simulations. The chain rigidity is tuned through the bending energy of adjacent polymer bonds, $U_{i,j} = kTK_{bend}(1-(\vec{n}_i \cdot \vec{n}_j))$, where $\vec{n}_i$ is the unit bond vector along the polymer backbone. The dynamic layer thickness is calculated from the spatial profile of the time-resolved data points of the collective intermediate dynamic structure factor $S_{col}(q,t,z)$. The static interfacial layer thickness is calculated from the spatial profile of the variance in density ($\rho(z) - \rho_b$).[2] A critical chain rigidity is found at around K_{bend} = 3 from the data. Adapted with permission from Carrillo *et al.*, Macromolecules **48**, 4207 (2015). Copyright 2015 American Chemical Society.

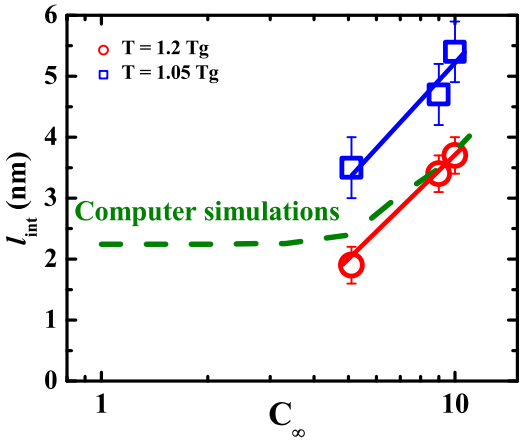

FIG. 14. Interfacial layer thickness, l_{int}, of the polymer nanocomposites from dielectric measurements with different chain rigidity. The dashed lines are results from computer simulations at high temperatures by assuming the bead size σ = 0.4 nm. The red circles are the results of dielectric measurements at T = 1.2 T_g and the blue squares are results at T = 1.05 T_g for PPG/SiO_2 (R_{NP} = 12.5 nm, φ_{NP} = 18 vol. %, C_∞ = 5.1), PVAc/SiO_2 (R_{NP} = 12.5 nm, φ_{NP} = 20.5 vol. %, C_∞ = 7.0), and P2VP/SiO_2 (R_{NP} = 15 nm, φ_{NP} = 26 vol. %, C_∞ = 10.0). Note the computer simulations and experiments match reasonably well at high temperatures and at large C_∞. Due to a lack of experimental data, it is difficult to validate the existence of a critical C_∞ as predicted in the computer simulations. For each polymer, l_{int} at low temperature close to T_g (T = 1.05 T_g) is systematically and significantly larger than l_{int} at high temperatures (T = 1.2 T_g), indicating a strong increase of l_{int} upon cooling.

Interestingly, the simulation also predicted the existence of a critical chain stiffness, above which the interfacial layer thickness starts to increase sharply with the chain rigidity (Figs. 13 and 14).

Detailed experimental studies on the role of chain rigidity have been performed very recently.[73] The authors analyzed SAXS, DSC, and BDS data to estimate the static and dynamic thickness of the interfacial layer in four different PNCs with the same loading of SiO_2 nanoparticles (Table I). They used a flexible polymer PPG, and semiflexible polymers PMMA, PVAc, and P2VP. All three experimental techniques employed provided consistent estimates of l_{int} (Table I). The results indeed revealed an increase in the interfacial layer thickness with the increase in the chain rigidity characterized by C_∞ especially at large $C_\infty > 5$ (Fig. 14). However, due to a lack of experimental data, it is difficult to validate the existence of a critical C_∞ as seen in the computer simulations. Nevertheless, chain rigidity clearly affects the thickness of the interfacial layer. At the same time the slowing down of segmental dynamics in the interfacial region seems to be less sensitive to the chain rigidity,[73] while it depends strongly on polymer-nanoparticle interactions.[33–35,74,75] Moreover, as shown in Table I and Fig. 14, l_{int} at low temperature close to T_g (T = 1.05 T_g) is systematically and significantly larger than l_{int} at high temperatures (T = 1.2 T_g) for different PNCs, indicating a strong increase of l_{int} upon cooling.

D. Role of molecular weight

The chain length, i.e., polymer molecular weight (MW) is another important parameter that affects properties of PNCs. It is expected that the thickness of the bound polymer layer should be comparable to the radius of gyration, R_g, of the polymer,[97–99] and thus would increase with increase in molecular weight. However, only a few studies on the influence of molecular weight on the interfacial layer structure and dynamics in PNCs have been performed.[47,50] Kim *et al.*[50] studied poly(ethylene glycol) (PEG)/silica nanocomposites with different molecular weights at relatively high temperatures by proton NMR. They found the volume of the interfacial polymer (a combination of the solid like layer and the immobilized layer in their terminology) slightly increases with molecular weight (Fig. 15). These results are consistent with expectations that the interfacial layer with slowing down in dynamics will be thicker for higher MW PNCs.[98,99] Interestingly, the thickness of the glassy layer, l_g, and the thickness of the immobile layer, l_{imm}, are almost identical for PEG/silica PNCs at T = 70 °C and T = 100 °C (Fig. 15), different from the observation in Fig. 14 and Table I. This discrepancy may come from the extremely high temperatures (T > T_g + 100 K) of the measurements of PEG/silica PNCs.

However, more recent studies on two different sets of polymer nanocomposites, PVAc/SiO_2 and P2VP/SiO_2, revealed an unexpected decrease in interfacial layer thickness and the change in dynamics with an increase in MW (Fig. 16).[47] This unexpected decrease appears in both BDS and DSC measurements: increasing MW leads to (i) a reduction in the broadening of the dielectric alpha relaxation peak (Fig. 16(a)) and (ii) to a reduction of the high temperature tail of the DSC step associated with the glass transition (Fig. 16(b)). The detailed SAXS studies and measurements of the samples' densities revealed a significant (~10%-15%) decrease in the density of the interfacial layer with increase in MW (Fig. 17(a)). At low MW the averaged density of the PNC matrix appears to be larger than that of the neat polymer, as expected for the attractive polymer-nanoparticle interactions. However, the ratio of the averaged matrix density in the PNC to the neat polymer

TABLE I. Summary of the interfacial layer thickness, l_{int}, from different techniques (data from Ref. 73). All samples include SiO_2 nanoparticles with radius R_{NP} ~ 12.5 nm; the numbers after the matrix name present the volume fraction of the nanoparticles. The values of C_∞ are taken from Refs. 95 and 96.

Sample	SAXS (nm)	TMDSC (nm)	BDS (T ~ 1.05 T_g) (nm)	BDS (T ~ 1.2 T_g) (nm)	AFM (nm)	C_∞
PPG/SiO_2-18 vol. %	1.3	1.8	3.5	1.9	N/A	5.1
PMMA/SiO_2-24 vol. %	2.3	2.1	N/A	N/A	N/A	7.0
PVAc/SiO_2-20.5 vol. %	2.32	2.4	4.7	3.4	3.0	9.4
P2VP/SiO_2-26 vol. %	4.7	3.4	5.4	3.7	N/A	10.0

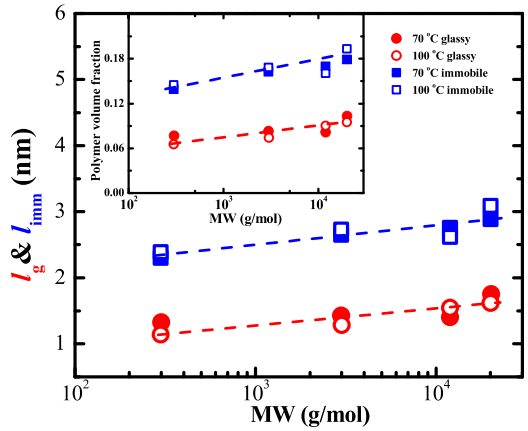

FIG. 15. Calculated glassy layer thickness (red), l_g, and the immobilized layer thickness (blue), l_{imm}, from NMR measurements of poly(ethylene glycol)/silica (R_{NP} = 22 nm, φ_{NP} = 40 vol. %) with different molecular weights at T = 70 °C (filled) and T = 100 °C (open). The calculation was carried out by assuming good dispersion of nanoparticles in polymer matrix. The inset shows the polymer fraction that belongs to the glassy layer (red) and the immobile layer (blue) from NMR. The inset data are adapted from Kim *et al.*, Macromolecules **45**(10), 4225–4237 (2012). Copyright 2012 under ACS Author Choice License.

density decreases with molecular weight and becomes less than one when chain size $2R_g$ becomes comparable to the interparticle surface-to-surface distance (Fig. 17(a) and its inset).[47] This unexpected MW effect does not vanish even upon extremely long time annealing ($\tau_{ann} \sim 10^{15}\ \tau_s$),[47] suggesting that it might be an equilibrium phenomenon or the system might be trapped in a very deep metastable state.

Detailed analysis of the BDS spectra demonstrated a clear decrease in the interfacial layer thickness (Fig. 17(b)), and a weaker change in the segmental relaxation time (Fig. 17(c)) for PNCs with higher MW. Based on these results and results of density and SAXS measurements, the authors[47] speculated that a frustration in long chain packing (Fig. 20) in the interfacial region can be the origin of the observed unexpected MW dependence (Figs. 16 and 17). The authors suggested that there are two competing processes that define the properties of the interfacial region: (i) the surface adsorption (the enthalpy effect) that slows down the motion of segments adjacent to the nanoparticles and (ii) the entropic effect caused by an increase of free volume due to frustrated chain packing in the interfacial layer that facilitates the segmental dynamics. Comparing the data for PEG/silica (Fig. 15) with P2VP/silica and PVAc/silica (Fig. 17) PNCs, we should pay attention to the much higher MWs studied in the latter case. The difference in conclusions of these two studies could also be caused by different methods used: NMR in the case of PEG/silica,[50] and BDS, DSC, and SAXS in the case of PVAc/silica and P2VP/silica.[47]

IV. DISCUSSION OF THE INTERFACIAL LAYER STRUCTURE, DYNAMICS, AND THEIR TEMPERATURE VARIATIONS IN PNCs

The presented overview of experimental studies clearly demonstrates that static structure (e.g., density), dynamics (e.g., segmental dynamics, T_g), and mechanical properties of PNCs are intrinsically heterogeneous and vary as a function of the distance from the nanoparticle surface. As a result, the interfacial layer with a gradient of various properties and a thickness l_{int} is formed. Using NMR data the authors of Ref. 24 suggested the existence of two different kinds of interfacial regions (Fig. 4): (i) the "glassy" or dynamically "dead" layer, and (ii) another "immobilized" layer with a reduced segmental mobility. However, the detailed dielectric studies and analysis of DSC data did not reveal any significant fraction of the "glassy" layer in several studied PNCs.[25,31,72] It appears that segmental dynamics in the interfacial layer can be slowed down by several orders of magnitude (Figs. 17(c) and 18), and the DSC data indicate that a fraction of the polymer has a $T_g \sim$ 30-40 K higher than the T_g of the neat polymer (Fig. 16(b)). However, no appreciable fraction of the composite appears to be "glassy" at temperatures high above T_g. It is obvious that the chain should be adsorbed to the nanoparticle surface for a very long time due to the high attractive nanoparticle-polymer interactions.[101–103] However, it does not mean that the segments at the interface are frozen. Whether the difference between NMR and BDS data interpretations reflects the difference in the accessible frequency range, or has some deeper physical reasons, remains to be resolved.

In any case, the estimates of the total interfacial layer thickness from various experimental techniques (SAXS, NMR, BDS, and DSC) provide consistent values in the range ~1.5-5 nm (Table I and Ref. 24). Very detailed studies

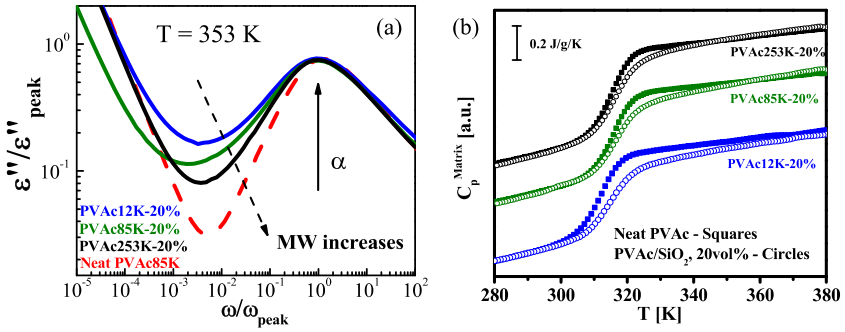

FIG. 16. (a) Normalized dielectric loss spectra, $\varepsilon''/\varepsilon''_{peak}$, of PVAc/$SiO_2$ (R_{NP} = 12.5 nm, φ_{NP} = 20 vol. %) nanocomposites with different molecular weight polymer matrices from MW = 12 kg/mol to 253 kg/mol. The dashed red line represents the dielectric spectra of the neat PVAc. The higher the MW, the lesser the effect of the nanoparticles is observed in the dielectric broadening. (b) Normalized specific heat capacity of polymer matrices, C_p^{mat}, of the same set of polymer nanocomposites as in panel (a). The circles represent the specific heat capacity of the PNCs and the squares represent the specific heat capacity of the corresponding neat polymer. The higher the MW, the lesser the effect of the nanoparticles is observed in the broadening of the glass transition step. Adapted from Cheng *et al.*, Phys. Rev. Lett. **116**(3), 038302 (2016). Copyright 2016 The American Physical Society.

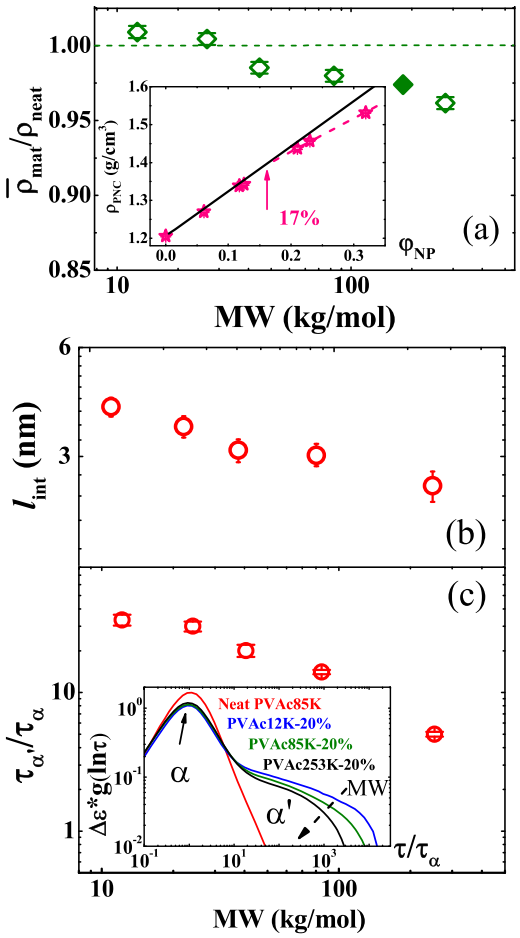

FIG. 17. (a) Relative mass density, $\bar{\rho}_{mat}/\rho_{neat}$, for PVAc/$SiO_2$ (R_{NP} = 12.5 nm, φ_{NP} = 20 vol. %) with different molecular weights. The filled symbols are a result of the re-analysis of the literature data[100] of PVAc/SiO_2 nanocomposites. The dashed line represents the average matrix density equal to the mass density of the neat polymer matrix. A decrease in average mass density of the matrix is found with increasing molecular weight. Moreover, the average mass density of the matrix is found to be smaller than the neat polymer matrix for MW larger than 30 kg/mol indicating a reduced mass density state of high MW PNCs. The inset shows the mass density for the PNC of different loadings of PVAc/SiO_2 (MW = 40 kg/mol, R_{NP} = 12.5 nm). The black solid line is a prediction from the TPM by assuming volume conservation. A deviation is found at around φ_{NP} = 17 vol. %, indicating the PNC with higher loadings have more free volume. (b) The interfacial layer thickness, l_{int}, and (c) the interfacial layer average slowing down, $\tau_{\alpha'}/\tau_{\alpha}$, of the PNCs as a function of MW. The inset in panel (c) represents the relaxation time distribution spectra of the bulk polymer and the interfacial layer polymer. A clear shoulder process, the interfacial layer process, can be identified from the spectra. Data were replotted from Cheng *et al.*, Phys. Rev. Lett. **116**(3), 038302 (2016). Copyright 2016 The American Physical Society.

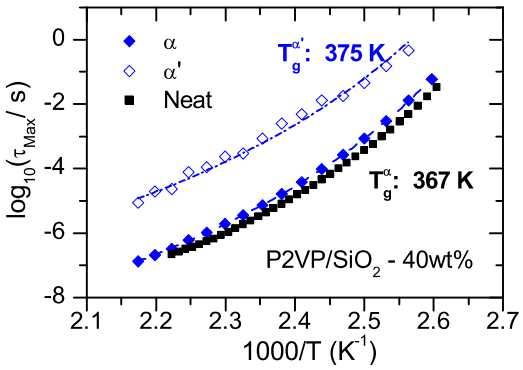

FIG. 18. The temperature dependence of the segmental relaxation time of the bulk polymer, τ_{α}, and the interfacial layer process, $\tau_{\alpha'}$, of P2VP/SiO_2-40 wt. % (MW = 101 kg/mol, R_{NP} = 12.5 nm). The filled black squares represent the temperature dependence of the neat P2VP with the same molecular weight. A significant slowing down and a large increase in the glass transition temperature in the interfacial layer process have been observed. However, the change in fragility of the interfacial layer is negligible. Adapted with permission from Holt *et al.*, Macromolecules **47**(5), 1837–1843 (2014). Copyright 2014 American Chemical Society.

combining experiment, theory, and atomistically detailed simulations have been performed on glycerol/silica nanocomposites.[31] Glycerol was specifically chosen instead of a polymer to remove additional complications related to long chain adsorption time, possible confinement effects of the chain squeezed between nanoparticles, and expected variations in entanglements. Experiments, theory, and simulations all provided consistent estimates of the interfacial layer thickness to be ~1.6-1.8 nm at high T.[31] This is in agreement with the estimates of l_{int} ~ 1.6-2.5 nm obtained for a thin glycerol films on a flat substrate.[104] The existence of the "glassy" layer was clearly excluded in this case.[31] Both experiment and theory also revealed that the slowing down of glycerol dynamics in the interfacial layer relative to the bulk glycerol increases upon cooling (Fig. 19(a)). This is consistent with the predictions of earlier simulations showing an increase in the fragility of segmental dynamics for attractive polymer-nanoparticle interactions.[33,34] BDS studies also revealed that the thickness of the interfacial layer in glycerol/silica nanocomposite increases from ~1.8 nm up to ~3.5 nm upon cooling from high T to T_g (Fig. 19(b)).[31] A significant increase in the thickness of the interfacial layer upon cooling has also been revealed in several PNCs (Figs. 14 and 19(b) and Table I). However, no significant increase in fragility has been found in these cases (see, e.g., Figs. 18 and 19(a)).[25,61]

To understand the mechanisms controlling the thickness of the interfacial layer in thin films and PNCs, several theoretical and simulation works have suggested that the interfacial layer thickness can be related to the length scale of dynamic heterogeneities ξ.[32,105] For example, based on the random first-order transition (RFOT) theory, authors of Ref. 105 suggested that l_{int} can be ~10-20 ξ. The analysis we have presented clearly contradicts this prediction, at least in the case of PNCs. It seems that the thickness of the interfacial layer appears to be of the order of the dynamic heterogeneity length scale, ξ ~ 1.5-4 nm.[106–109] A similar conclusion has been achieved also from analysis of simulations results based on the string-like motion approach.[32,33,110] The observed increase in the interfacial layer thickness upon approaching T_g (Figs. 14 and 19(b) and Table I) is consistent with the expected increase in the dynamic heterogeneity/cooperativity length scale on cooling. It remains important to unravel a possible relationship of the dynamic heterogeneity length scale ξ and the thickness of the interfacial layer l_{int}.[32] The complication here is related to the challenge of experimental measurements of the dynamic heterogeneity length scale.

The presented above results also revealed that structure, thickness, and dynamics of the interfacial layer can be strongly affected by the molecular weight of the polymer (Figs. 15–17). It seems that when the size of the chain ($2R_g$) becomes comparable to the distance between nanoparticle surfaces d_{IPS},

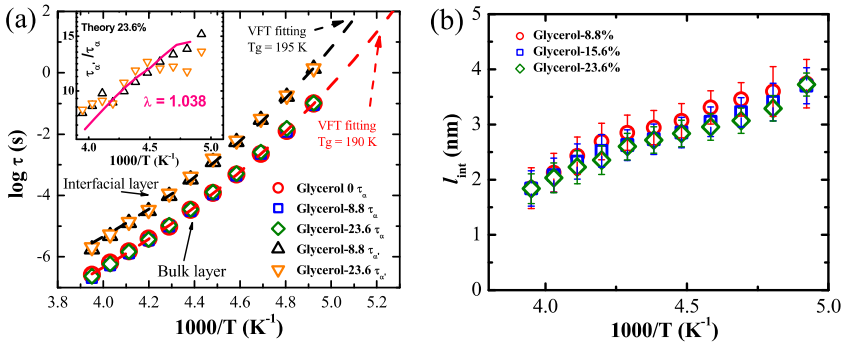

FIG. 19. (a) The temperature dependence of the characteristic segmental relaxation time of the bulk glycerol, τ_α, and the interfacial layer glycerol, $\tau_{\alpha\prime}$ in a set of glycerol/SiO_2 nanocomposites (R_{NP} = 12.5 nm). A significant slowing down in the segmental relaxation time is found for the interfacial layer glycerol. The inset shows the temperature dependence of the interfacial layer slowing down, $\tau_{\alpha\prime}/\tau_\alpha$, where the interfacial layer slowing down increases from ~8 to ~16 with cooling from 253 K to 208 K. The solid pink line is a prediction from the elastic collective nonlinear Langevin equation (ECNLE) theory with a fixed first absorbed layer densification parameter λ = 1.038. Data replotted from J. Chem. Phys. **143**(19), 194704 (2015). Copyright 2015 AIP Publishing LLC. (b) The temperature dependence of the interfacial layer thickness, l_{int} (T), of glycerol/SiO_2 nanocomposites with different loadings. The data show little effects of loading to the interfacial layer thickness on the loading ranges under study. The numbers 0, 8.8, and 23.6 indicate the volume fraction of silica nanoparticles as 0 vol. %, 8.8 vol. %, and 23.6 vol. %, respectively, in both panels (a) and (b). Adapted with permission from J. Chem. Phys. **143**(19), 194704 (2015). Copyright 2015 AIP Publishing LLC.

frustration in packing of long chains in the interfacial region leads to a significant reduction in density[43,47,100] (Fig. 17(a)). It was suggested that short chains can pack better at the interface, and also that nanocomposites with short chains have a sufficient amount of non-adsorbed chains. The latter can easily penetrate the interfacial region and increase density (Fig. 20). In contrast, long chains form a layer with frustrated chain packing and almost all the chains are adsorbed to nanoparticles in composites with high MW polymers.[47] All these factors restrict the packing of long chains and lead to lower density in the interfacial layer. It remains a challenge to understand how the polymer regions with larger free volume (lower density) still exhibit slower dynamics (Fig. 17). It has been suggested theoretically[111] that the slowing down might be affected by chain stretching in the interfacial region. As was discussed in Ref. 36, the idea of chain stretching is consistent with significant enhancement of mechanical moduli in the interfacial layer even in a glassy state. So, it is possible that a balance between chain stretching and density variations controls the slowing down of segmental dynamics in the interfacial region. It also remains a puzzle whether the observed decrease in density of the interfacial layer of high molecular weight PNCs is an equilibrium state, or if long enough annealing will result in a denser state. Detailed theoretical and computational studies might help resolve these questions.

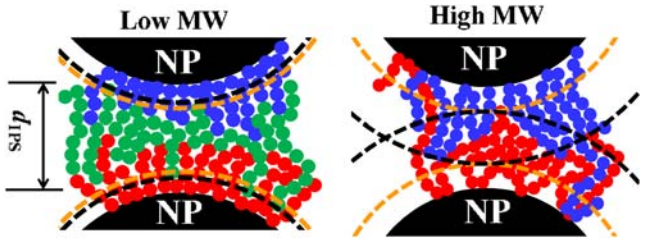

FIG. 20. Proposed mechanism for the chain packing in polymer nanocomposites with different molecular weights. The d_{IPS} is the average interparticle surface-to-surface distance. Left: low MW chains, $d_{IPS} > 2R_g$, tend to pack densely at the interface (red chains and blue chains) due to the low enthalpic and entropic penalty. The large number of free chains (green chains) also facilitates the chain packing at the interface. Right: high MW chains, $d_{IPS} \leq 2R_g$, tend to form long loops and long tails that bridge adjacent nanoparticles. Conformational changes of long chains need to overcome the large enthalpic and entropic barrier. In this case, loop-loop repulsion dominates the packing process and frustrated chain packing forms. Detailed description of the mechanism can be found in Cheng *et al.*, Phys. Rev. Lett. **116**(3), 038302 (2016). Copyright 2016 The American Physical Society.

V. CONCLUSIONS AND FUTURE PERSPECTIVES

Progress during this decade has led to developments of robust experimental techniques to study structure and dynamics of the interfacial layer in polymer nanocomposites. SAXS and SANS provide estimates of the interfacial layer thickness and its density. However, there were no systematic studies of the temperature dependence of the interfacial region in PNCs using these scattering techniques. It would be also important to provide experimental analysis of the chain stretching in the interfacial region, and to verify the theoretical predictions of chain stretching.[111] These structural studies might help us better understand the role of density variations and chain stretching in tuning the structure and dynamics of the interfacial region. The changes in dynamics of the interfacial region can be well studied using NMR, BDS, and DSC techniques. The first two can also provide analysis of the interfacial dynamics as a function of temperature.

Analysis of experimental and computational data suggests that the slowing down of the interfacial dynamics depends mostly on the strength of the polymer-nanoparticle interactions, while the thickness of the interfacial layer depends mostly on the chain rigidity.[35] It remains an open challenge to verify the proposed relationship between the thickness of the interfacial layer and the characteristic length scale of dynamic heterogeneities. Both of them are in the range of several nanometers, and both increase upon approaching T_g. However, the thickness of the interfacial layer in PNCs is also affected by the polymer molecular weight and by the nanoparticle size. Systematic studies of the role of nanoparticle size, especially in the regime of small nanoparticles,[112] $R_{NP} << R_g$, should provide better understanding of how the surface curvature affects

the interfacial layer structure and dynamics. Do we even have any interfacial region in this extreme case?[112] Or can small sticky nanoparticles be considered as temporary crosslinks? Another interesting question in this case is how long is the chain adsorption time for the attractive nanoparticles? And how does it depend on the ratio between R_{NP} and R_g? Chain adsorption/desorption time drastically affects the viscoelastic properties and flow of the PNCs at high temperatures.

In this focus article, we intentionally limited the discussion of composites with attractive spherical nanoparticles providing physical adsorption of chains. We did not discuss composites with "hairy" nanoparticles (i.e., nanoparticles with grafted chains). Grafting of chains strongly improves nanoparticle dispersion and might lead to formation of some ordered structures.[27,41,81] However, not many papers have focused on the analysis of the interfacial layer properties in this class of nanocomposites. Studies have revealed some similarities and differences with the interfacial dynamics in the case of physically adsorbed chains.[46] Also, there are many PNCs with two-dimensional (e.g., graphene-base and clays)[15,113] and one dimensional (e.g., carbon nanotubes) nanofillers.[114] Unfortunately, the rich literature focused on these types of PNCs has many controversies and confusions, most probably related to complications with nanofiller aggregations. Developments of model composites with good dispersion of 2-D and/or 1-D nanofillers will allow quantitative analysis of the interfacial regions also in these materials.

Another important direction is the unraveling of the relationship between the interfacial region's characteristics and the macroscopic properties of PNCs. Developing more accurate models that account for the gradient of properties in the interfacial region is needed for the proper description of the macroscopic properties and for the design of PNCs with desired properties.

The question of high practical importance that we did not discuss in this paper is how the interfacial layer properties affect the flow behavior and processibility of PNCs. This complicated question is related to the long time diffusion behavior of polymers and nanoparticles in PNCs. Examples from recent works by Karen Winey and co-workers[115,116] revealed that the presence of the adsorbed polymer layer increases the effective size of nanoparticles. This affects significantly the diffusion of both the polymer and nanoparticles. However, the role of the interfacial layer (that is different from the adsorbed layer) in the diffusion and processing behavior of PNCs remains unknown and requires additional studies.

The last point we want to comment on is the analogy between PNCs and thin films that is emphasized in many articles.[29,40] Indeed, the behavior of polymeric materials in the interfacial region is similar for thin supported films and PNCs. However, this analogy should be taken with some precaution. First of all, at sufficient loading, when the distance between nanoparticle surfaces becomes comparable to the chain size, $d_{IPS} \sim 2R_g$, the confinement effect becomes important in PNCs. In that case it might be analogous to the behavior of polymer in capped films or in confinement. Also, the size of the nanoparticles and their surface curvature play a role in PNCs but have no analogy in thin films. Nevertheless, many ideas and results obtained in the field of PNCs can be applied to thin films and vice versa.

ACKNOWLEDGMENTS

This work was supported by the U.S. Department of Energy, Office of Science, Basic Energy Sciences, Materials Science & Engineering Division.

[1] A. C. Balazs, T. Emrick, and T. P. Russell, Science **314**, 1107 (2006).
[2] V. Mittal, *Modeling and Prediction of Polymer Nanocomposite Properties* (Wiley-VCH, 2013).
[3] J. Jancar, J. F. Douglas, F. W. Starr, S. K. Kumar, P. Cassagnau, A. J. Lesser, S. S. Sternstein, and M. J. Buehler, Polymer **51**, 3321 (2010).
[4] L. S. Schadler, S. K. Kumar, B. C. Benicewicz, S. L. Lewis, and S. E. Harton, MRS Bull. **32**, 335 (2007).
[5] S. S. Ray and M. Okamoto, Prog. Polym. Sci. **28**, 1539 (2003).
[6] R. A. Vaia and E. P. Giannelis, MRS Bull. **26**, 394 (2001).
[7] L. L. Beecroft and C. K. Ober, Chem. Mater. **9**, 1302 (1997).
[8] S. Li, M. Meng Lin, M. S. Toprak, D. K. Kim, and M. Muhammed, Nano Rev. **1**, 5214 (2010).
[9] D. V. Szabó and T. Hanemann, in *Advances in Polymer Nanocomposites* (Woodhead Publishing, 2012), p. 567.
[10] R. M. Mutiso and K. I. Winey, Prog. Polym. Sci. **40**, 63 (2015).
[11] H. Ning, M. Zen, Y. Cheng, Y. Go, F. Hisao, and H. Toshiyuki, Nanotechnol. **19**, 215701 (2008).
[12] S. C. Tjong, Mater. Sci. Eng., R **53**, 73 (2006).
[13] A. J. Crosby and J. Y. Lee, Polym. Rev. **47**, 217 (2007).
[14] T. C. Merkel, B. D. Freeman, R. J. Spontak, Z. He, I. Pinnau, P. Meakin, and A. J. Hill, Science **296**, 519 (2002).
[15] D. R. Paul and L. M. Robeson, Polymer **49**, 3187 (2008).
[16] R. Krishnamoorti, MRS Bull. **32**, 341 (2007).
[17] G. D. Smith and D. Bedrov, Langmuir **25**, 11239 (2009).
[18] L. M. Hall, A. Jayaraman, and K. S. Schweizer, Curr. Opin. Solid State Mater. Sci. **14**, 38 (2010).
[19] L. M. Hall, B. J. Anderson, C. F. Zukoski, and K. S. Schweizer, Macromolecules **42**, 8435 (2009).
[20] L. M. Hall and K. S. Schweizer, J. Chem. Phys. **128**, 234901 (2008).
[21] N. Jouault, D. Zhao, and S. K. Kumar, Macromolecules **47**, 5246 (2014).
[22] D. Zhao, D. Schneider, G. Fytas, and S. K. Kumar, ACS Nano **8**, 8163 (2014).
[23] J. Berriot, H. Montes, F. Martin, M. Mauger, W. Pyckhout-Hintzen, G. Meier, and H. Frielinghaus, Polymer **44**, 4909 (2003).
[24] A. Papon, H. Montes, F. Lequeux, J. Oberdisse, K. Saalwachter, and L. Guy, Soft Matter **8**(15), 4090–4096 (2012).
[25] A. P. Holt, P. J. Griffin, V. Bocharova, A. L. Agapov, A. E. Imel, M. D. Dadmun, J. R. Sangoro, and A. P. Sokolov, Macromolecules **47**(5), 1837–1843 (2014).
[26] S. Gong, Q. Chen, J. F. Moll, S. K. Kumar, and R. H. Colby, ACS Macro Lett. **3**, 773–777 (2014).
[27] S. K. Kumar, N. Jouault, B. Benicewicz, and T. Neely, Macromolecules **46**, 3199 (2013).
[28] S. K. Kumar and R. Krishnamoorti, Annu. Rev. Chem. Biomol. Eng. **1**, 37 (2010).
[29] P. Rittigstein, R. D. Priestley, L. J. Broadbelt, and J. M. Torkelson, Nat. Mater. **6**, 278 (2007).
[30] J. Moll and S. K. Kumar, Macromolecules **45**, 1131 (2012).
[31] S. Cheng, S. Mirigian, J.-M. Y. Carrillo, V. Bocharova, B. G. Sumpter, K. S. Schweizer, and A. P. Sokolov, J. Chem. Phys. **143**(19), 194704 (2015).
[32] P. Z. Hanakata, J. F. Douglas, and F. W. Starr, Nat. Commun. **5**, 4163 (2014).
[33] B. A. Pazmino Betancourt, J. F. Douglas, and F. W. Starr, Soft Matter **9**, 241 (2013).
[34] F. W. Starr and J. F. Douglas, Phys. Rev. Lett. **106**, 115702 (2011).
[35] J.-M. Y. Carrillo, S. Cheng, R. Kumar, M. Goswami, A. P. Sokolov, and B. G. Sumpter, Macromolecules **48**, 4207 (2015).
[36] S. Cheng, V. Bocharova, A. Belianinov, S. Xiong, A. Kisliuk, S. Somnath, A. P. Holt, O. S. Ovchinnikova, S. Jesse, H. Martin, T. Etampawala, M. Dadmun, and A. P. Sokolov, Nano Lett. **16**(6), 3630–3637 (2016).
[37] M. Krutyeva, A. Wischnewski, M. Monkenbusch, L. Willner, J. Maiz, C. Mijangos, A. Arbe, J. Colmenero, A. Radulescu, O. Holderer, M. Ohl, and D. Richter, Phys. Rev. Lett. **110**, 108303 (2013).

[38]J. Berriot, H. Montes, F. Lequeux, D. Long, and P. Sotta, "Gradient of glass transition temperature in filled elastomers," Europhys. Lett. **64**, 50 (2003).
[39]J. Berriot, H. Montes, F. Lequeux, D. Long, and P. Sotta, Macromolecules **35**, 9756 (2002).
[40]A. Bansal, H. C. Yang, C. Z. Li, K. W. Cho, B. C. Benicewicz, S. K. Kumar, and L. S. Schadler, Nat. Mater. **4**, 693 (2005).
[41]P. Akcora, H. Liu, S. K. Kumar, J. Moll, Y. Li, B. C. Benicewicz, L. S. Schadler, D. Acehan, A. Z. Panagiotopoulos, V. Pryamitsyn, V. Ganesan, J. Ilavsky, P. Thiyagarajan, R. H. Colby, and J. F. Douglas, Nat. Mater. **8**, 354 (2009).
[42]K. Nusser, S. Neueder, G. J. Schneider, M. Meyer, W. Pyckhout-Hintzen, L. Willner, A. Radulescu, and D. Richter, Macromolecules **43**, 9837 (2010).
[43]N. Jouault and J. Jestin, ACS Macro Lett. **5**, 1095 (2016).
[44]N. Jouault, M. K. Crawford, C. Chi, R. J. Smalley, B. Wood, J. Jestin, Y. B. Melnichenko, L. He, W. E. Guise, and S. K. Kumar, ACS Macro Lett. **5**(4), 523–527 (2016).
[45]A. Guinier and G. Fournet, *Small-Angle Scattering of X-Rays* (John Wiley and Sons, New York, 1955).
[46]A. P. Holt, V. Bocharova, S. Cheng, A. M. Kisliuk, B. T. White, T. Saito, D. Uhrig, J. P. Mahalik, R. Kumar, A. E. Imel, T. Etampawala, H. Martin, N. Sikes, B. G. Sumpter, M. D. Dadmun, and A. P. Sokolov, ACS Nano **10**, 6843 (2016).
[47]S. Cheng, A. P. Holt, H. Wang, F. Fan, V. Bocharova, H. Martin, T. Etampawala, B. T. White, T. Saito, N.-G. Kang, M. D. Dadmun, J. W. Mays, and A. P. Sokolov, Phys. Rev. Lett. **116**(3), 038302 (2016).
[48]S. Kaufman, W. P. Slichter, and D. D. Davis, J. Polym. Sci., Part A-2 **9**, 829 (1971).
[49]J. Berriot, F. Lequeux, L. Monnerie, H. Montes, D. Long, and P. Sotta, J. Non-Cryst. Solids **307–310**, 719–724 (2002).
[50]S. Y. Kim, H. W. Meyer, K. Saalwächter, and C. F. Zukoski, Macromolecules **45**(10), 4225–4237 (2012).
[51]G. Tsagaropoulos and A. Eisenburg, Macromolecules **28**(1), 396–398 (1995).
[52]G. Tsagaropoulos and A. Eisenberg, Macromolecules **28**, 6067 (1995).
[53]M. Qu, F. Deng, S. M. Kalkhoran, A. Gouldstone, A. Robisson, and K. J. Van Vliet, Soft Matter **7**, 1066 (2011).
[54]S. Aoyama, Y. T. Park, C. W. Macosko, T. Ougizawa, and G. Haugstad, Langmuir **30**, 12950 (2014).
[55]K.-H. Liao, S. Aoyama, A. A. Abdala, and C. Macosko, Macromolecules **47**, 8311 (2014).
[56]D. Wang, S. Fujinami, K. Nakajima, K.-i. Niihara, S. Inukai, H. Ueki, A. Magario, T. Noguchi, M. Endo, and T. Nishi, Carbon **48**, 3708 (2010).
[57]W. Xia, J. Song, D. D. Hsu, and S. Keten, Macromolecules **49**, 3810 (2016).
[58]G. Maurice, D. Rouxel, B. Vincent, R. Hadji, J.-F. Schmitt, M. Taghite, and R. Rahouadj, Polym. Eng. Sci. **53**, 1502 (2013).
[59]P. Voudouris, J. Choi, N. Gomopoulos, R. Sainidou, H. Dong, K. Matyjaszewski, M. R. Bockstaller, and G. Fytas, ACS Nano **5**, 5746 (2011).
[60]F. Kremer and A. Schohals, *Broadband Dielectric Spectroscopy* (Springer-Verlag, Berlin, 2002).
[61]M. Füllbrandt, P. J. Purohit, and A. Schönhals, Macromolecules **46**, 4626 (2013).
[62]D. Fragiadakis, P. Pissis, and L. Bokobza, Polymer **46**, 6001 (2005).
[63]D. Fragiadakis, P. Pissis, and L. Bokobza, J. Non-Cryst. Solids **352**, 4969 (2006).
[64]P. A. M. Steeman and F. H. J. Maurer, Colloid Polym. Sci. **268**, 315 (1990).
[65]R. Richert, Annu. Rev. Phys. Chem. **62**, 65 (2011).
[66]A. Triolo, F. Lo Celso, F. Negroni, V. Arrighi, H. Qian, R. E. Lechner, A. Desmedt, J. Pieper, B. Frick, and R. Triolo, Appl. Phys. A **74**, s490 (2002).
[67]V. Arrighi, J. S. Higgins, A. N. Burgess, and G. Floudas, Polymer **39**, 6369 (1998).
[68]G. J. Schneider, K. Nusser, L. Willner, P. Falus, and D. Richter, Macromolecules **44**, 5857 (2011).
[69]M. Lungova, M. Krutyeva, W. Pyckhout-Hintzen, A. Wischnewski, M. Monkenbusch, J. Allgaier, M. Ohl, M. Sharp, and D. Richter, Phys. Rev. Lett. **117**, 147803 (2016).
[70]G. J. Schneider, K. Nusser, S. Neueder, M. Brodeck, L. Willner, B. Farago, O. Holderer, W. J. Briels, and D. Richter, Soft Matter **9**, 4336 (2013).
[71]A. Sargsyan, A. Tonoyan, S. Davtyan, and C. Schick, Eur. Polym. J. **43**, 3113 (2007).
[72]G. P. Baeza, C. Dessi, S. Costanzo, D. Zhao, S. Gong, A. Alegria, R. H. Colby, M. Rubinstein, D. Vlassopoulos, and S. K. Kumar, Nat. Commun. **7**, 11368 (2016).
[73]S. Cheng, B. Carroll, W. Lu, F. Fan, J.-M. Y. Carrillo, H. Martin, A. P. Holt, N.-G. Kang, V. Bocharova, J. W. Mays, B. G. Sumpter, M. Dadmun, and A. P. Sokolov, "Interfacial properties of polymer nanocomposites: Role of chain rigidity and dynamic heterogeneity length scale," Macromolecules (published online, 2017).
[74]F. W. Starr, T. B. Schrøder, and S. C. Glotzer, Macromolecules **35**, 4481 (2002).
[75]F. W. Starr, T. B. Schrøder, and S. C. Glotzer, Phys. Rev. E **64**, 021802 (2001).
[76]A. Papon, K. Saalwächter, K. Schäler, L. Guy, F. Lequeux, and H. Montes, Macromolecules **44**, 913 (2011).
[77]K. U. Kirst, F. Kremer, and V. M. Litvinov, Macromolecules **26**, 975 (1993).
[78]V. M. Litvinov and H. W. Spiess, Die Makromol. Chem. **192**, 3005 (1991).
[79]V. M. Litvinov and P. A. M. Steeman, Macromolecules **32**, 8476 (1999).
[80]D. Maillard, S. K. Kumar, A. Rungta, B. C. Benicewicz, and R. E. Prud'homme, Nano Lett. **11**, 4569 (2011).
[81]S. Srivastava, P. Agarwal, and L. A. Archer, Langmuir **28**, 6276 (2012).
[82]D. S. Simmons, Macromol. Chem. Phys. **217**, 137 (2016).
[83]Y. Song and Q. Zheng, Prog. Mater. Sci. **84**, 1 (2016).
[84]G. Allegra, G. Raos, and M. Vacatello, Prog. Polym. Sci. **33**, 683 (2008).
[85]K. I. Skau and E. M. Blokhuis, Eur. Phys. J. E **7**, 13 (2002).
[86]C.-H. Lin, Y.-C. Tsai, and C.-K. Hu, Phys. Rev. E **75**, 031903 (2007).
[87]E. Hershkovits, A. Tannenbaum, and R. Tannenbaum, J. Phys. Chem. C **111**, 12369 (2007).
[88]J. Choi, H. Shin, S. Yang, and M. Cho, Compos. Struct. **119**, 365 (2015).
[89]L. J. Fetters, D. J. Lohse, D. Richter, T. A. Witten, and A. Zirkel, Macromolecules **27**, 4639 (1994).
[90]L. J. Fetters, D. J. Lohse, and R. H. Colby, in *Physical Properties of Polymers Handbook*, edited by J. Mark (Springer, New York, 2007), p. 447.
[91]A. Yethiraj, J. Chem. Phys. **101**, 2489 (1994).
[92]E. Y. Kramarenko, R. G. Winkler, P. G. Khalatur, A. R. Khokhlov, and P. Reineker, J. Chem. Phys. **104**, 4806 (1996).
[93]T. Sintes, K. Sumithra, and E. Straube, Macromolecules **34**, 1352 (2001).
[94]P. Linse and N. Källrot, Macromolecules **43**, 2054 (2010).
[95]S. M. Aharoni, Macromolecules **16**, 1722 (1983).
[96]A. Shizuo, Bull. Chem. Soc. Jpn. **39**, 434 (1966).
[97]P. G. de Gennes, Adv. Colloid Interface Sci. **27**, 189 (1987).
[98]O. Guiselin, Europhys. Lett. **17**, 225 (1992).
[99]J. M. H. M. Scheutjens and G. J. Fleer, J. Phys. Chem. **84**, 178 (1980).
[100]R. B. Bogoslovov, C. M. Roland, A. R. Ellis, A. M. Randall, and C. G. Robertson, Macromolecules **41**, 1289 (2008).
[101]C. Housmans, M. Sferrazza, and S. Napolitano, Macromolecules **47**, 3390 (2014).
[102]S. Napolitano, S. Capponi, and B. Vanroy, Eur. Phys. J. E **36**, 61 (2013).
[103]S. Napolitano and M. Wubbenhorst, Nat. Commun. **2**, 260 (2011).
[104]S. Capponi, S. Napolitano, N. R. Behrnd, G. Couderc, J. Hulliger, and M. Wübbenhorst, J. Phys. Chem. C **114**, 16696 (2010).
[105]J. D. Stevenson and P. G. Wolynes, J. Chem. Phys. **129**, 234514 (2008).
[106]X. H. Qiu and M. D. Ediger, J. Phys. Chem. B **107**, 459 (2003).
[107]L. Hong, V. N. Novikov, and A. P. Sokolov, J. Non-Cryst. Solids **357**, 351 (2011).
[108]L. Hong, P. D. Gujrati, V. N. Novikov, and A. P. Sokolov, J. Chem. Phys. **131**, 194511 (2009).
[109]U. Tracht, M. Wilhelm, A. Heuer, H. Feng, K. Schmidt-Rohr, and H. W. Spiess, Phys. Rev. Lett. **81**, 2727 (1998).
[110]F. W. Starr, J. F. Douglas, and S. Sastry, J. Chem. Phys. **138**, 12A541 (2013).
[111]F. T. Oyerokun and K. S. Schweizer, J. Chem. Phys. **123**, 224901 (2005).
[112]S. Cheng, S.-J. Xie, J.-M. Y. Carrillo, B. Carroll, H. Martin, P.-F. Cao, M. D. Dadmun, B. G. Sumpter, V. N. Novikov, K. S. Schweizer, and A. P. Sokolov, ACS Nano **11**, 752 (2017).
[113]T. Kuilla, S. Bhadra, D. Yao, N. H. Kim, S. Bose, and J. H. Lee, Prog. Polym. Sci. **35**, 1350 (2010).
[114]Z. Spitalsky, D. Tasis, K. Papagelis, and C. Galiotis, Prog. Polym. Sci. **35**, 357 (2010).
[115]P. J. Griffin, V. Bocharova, L. R. Middleton, R. J. Composto, N. Clarke, K. S. Schweizer, and K. I. Winey, ACS Macro Lett. **5**, 1141 (2016).
[116]J. Choi, M. J. A. Hore, J. S. Meth, N. Clarke, K. I. Winey, and R. J. Composto, ACS Macro Lett. **2**, 485 (2013).